Supporting Information

Moriel-Carretero et al. 10.1073/pnas.1107425108

SI Materials and Methods

Strains and Plasmids. Strains used in this study are described in Table S1. The strain bearing the *YDJ1* deletion that was used for most experiments derives from Y03012 after repeated backcrosses with YBP250. Other double mutants have been obtained after mating the indicated parental strains. MMIV-5 was obtained by disruption of *YDJ1* in SC0946 with a NAT-resistance cassette. MMIV-17 was obtained by integration of a FLAG-tag followed by a KAN-resistance cassette before the stop codon of the *YDJ1* ORF. Plasmids pWJ1344 carrying the Rad52-YFP construct (1), pLAUR (2), pG/ER(G) containing the hER ORF (3), and pUCΔSS- ERE containing the reporter gene *lacZ* under the ERE (4) have been previously described.

Recombination Analyses. Recombination was determined by using the chromosomal direct-repeat system *his3-Δ5′::his3-Δ3′* (5) to measure unequal sister chromatid exchange. Each recombination frequency was obtained as the mean value of three median recombination frequencies obtained each from six independent colonies. For UV-induced frequencies, cells were plated on selective medium for recombinants, irradiated in an UV irradiation chamber (Dr. Gröbel UV-Elektronik) and cultured for 3 d in darkness.

Exponential cultures grown in the appropriate medium were used to generate 10-fold serial dilutions in distilled sterile water. Serial dilutions were later plated onto selective media (for transcriptional assays) or YPAD plates supplemented with drugs (for sensitivity assays). When necessary, dried plates were irradiated in an UV irradiation chamber (Dr. Gröbel UV-Elektronik) with the indicated doses. Survival curves were calculated at each point as the percentage of surviving colonies after irradiation with each dose growing on YPAD plates, in which an appropriate dilution had been spread, versus the number of colonies arising on nonirradiated plates.

Spontaneous and UV-Induced Rad52 Foci. Nuclei from midlog cells bearing plasmid pWJ1344 and grown in SC-leu were stained with DAPI and Rad52 foci were counted in S-G2 cells. For UV-induced Rad52 foci, cells were resuspended in water in Petri dishes as a 4-mm-deep cell suspension, UV-irradiated, and incubated in SC-leu for a further 2 h before foci inspection.

FACS Analysis. One milliliter of the desired culture was centrifuged and washed with 1 mL distilled water, then resuspended in 1 mL 70% ethanol. Cells were washed with 1 mL 1× PBS solution, resuspended in 100 μL 1× PBS–RNase 1 mg/mL, and left for overnight incubation. Next, they were washed again with 1× PBS solution and resuspended in 1 mL of 5 μg/mL propidium iodide in 1× PBS solution, incubated in darkness for 30 min, sonicated 3 s at 10% amplitude, and scored in a FACScalibur device (Becton Dickinson).

Northern Analysis. Northern analysis was performed as previously described (6). The *GAL1* signal was detected by using a probe against the full *GAL1* ORF and values normalized with respect to the 28S rRNA values. Signals were quantified by using a PhosphorImager (FLA-5100; Fujifilm) and ImageGauge software.

Strains were cultured up to $0.7_{OD600nm}$ in SC (synthetic complete medium with 2% glucose), centrifuged, washed twice, and diluted to $0.2_{O.D.600nm}$ in SGL (synthetic complete medium with 2% glycerol-2% lactate) overnight. A 50-mL sample was then saved as noninduced and glucose or galactose was added to a 2% final concentration. Samples (50 mL) were taken at the indicated time points. Samples processing was performed as described (7). IgG Sepharose (GE Healthcare) was incubated with samples overnight to precipitate TAP-tagged Rad3. To precipitate Ydj1-FLAG or total RNA polymerase II, samples were incubated overnight with anti-FLAG antibody (F3165; Sigma) or anti-RNA polymerase II 8WG16 antibody (Covance), respectively. In these two latter cases, samples were incubated the next morning with protein A Sepharose (GE Healthcare) for at least 4 h. The Wizard SV DNA clean-up system (Promega) was used for the last DNA purification step. Quantitative PCR was performed against the *GAL1* locus promoter (coordinates 278969–279048 on chromosome II). Normalization was done with values of amplification at *ARS504* (coordinates 9754–9837 on chromosome V), a location free from transcription.

Estrogen Receptor Phosphorylation Kinetics. WT, *kin28-ts16*, and *ydj1Δ* strains were grown in minimal medium selecting for plasmids pG/ER(G) and pUCΔSS-ERE until the exponential phase. A sample indicative of basal ER state (time 0) was taken, and β-estradiol was added to a final concentration of 0.1 μM. Time points were taken to follow ER phosphorylation kinetics.

Western Blots. For ER protein abundance and phosphorylation, TCA-extracted proteins were separated in 10% PAGE. Membranes were blocked in 1× TBS 5% 0.05% Tween milk. Antibodies anti-ERα (ab2746; Abcam) and anti-ER$_{Ser118-P}$ (ab32396; Abcam) were incubated in the same buffer at a 1:1,000 dilution for 3 h and 90 min, respectively. For TFIIH components, the following primary antibodies were used at the indicated dilutions: anti-Ssl1 (1:500), anti-TAP for Rad3 and Tfb4 detection in Fig. 4*A* (1:2,000; Thermo Scientific), all in blocking reagent (Roche); anti-Tfb2 (1:1,000) as well as anti-Tfb4 (1:1,000), anti-Rad3 (1:300, sc-11963; Santa Cruz Biotechnology), and anti-Rad14 (1:1,000, ab22092; Abcam) for detection in Fig. 4*A* were incubated in 1× TBS 0.05% Tween 5% milk for 1 h. Anti-Ssl1, anti-Tfb2, and anti-Tfb4 were a gift from Yuichiro Takagi. Anti-actin (ab8224; Abcam) was used at a 1:1,000 dilution in 1× TBS 0.05% Tween 5% milk for 1 h. Secondary antibody was a horseradish peroxidase-conjugated anti-rabbit or anti-mouse or anti-goat IgG antibody (Sigma and Santa Cruz Biotechnology) were incubated in the same buffer as primary antibodies for 1 h. SuperSignal West Pico chemiluminescent substrate (Pierce) was added to the blots, and the chemiluminescent signal was detected using a BioMax light film (Kodak).

TAP-Tagged Purification of TFIIH. Yeast strains CB010-TFB4 and MMIII-60 (*ydj1Δ*) were grown in 2 L of 2× YPD (4% (wt/vol) Bacto Peptone, 2% (wt/vol) yeast extract, 4% (wt/vol) glucose up to 3 to $4_{OD600nm}$. Cells were harvested and washed once with cold water, and the resulting pellets were extruded into liquid nitrogen. The purification was performed essentially as previously described (8). The Tfb4-TAP protein was isolated from yeast lysates by affinity purification by using an IgG-Sepharose column (GE Healthcare). Proteins in the various elution fractions were concentrated with trichloroacetic acid, resolved by 10% SDS/PAGE, and Coomassie-stained for visualization. Proteins were identified by using MALDI-TOF MS identification.

Bioinformatics. Proteins sequences were obtained from the PubMed database and aligned by using the ClustalW and the LAlign tools (EBI). The Tfb2-Tfb5 crystal structure has been previously published (9). Molecules were processed by using RasMol.

Statistical Analysis. The six motif-containing TFIIH proteins were assigned a letter, indicative of a category (Tfb5, A; Tfb4, B; Ssl1, C; Tfb2, D; Rad3, E; Rad25, F), whose features were the number of amino acids aligned between the *S. cerevisiae* and the human proteins, as well as their degree of identity and of similarity. These three features were used to choose other proteins that, upon alignment, kept essentially the same values. For this, the number of identical or similar amino acids being aligned was calculated. Proteins were randomly chosen except for the criterion that they had no reported interaction with Ydj1, to minimize the presence of motives caused by real interaction with the chaperone. Three random groups containing one protein belonging to each category from A to F were created. We created nominal categories by separating proteins depending on the aligned number of amino acids. The presence of motives for each class was noted. Seen that random control groups displayed a similar distribution of motif frequency between them, from that moment on all data were fused as a single control group. The

number of conserved motives found in proteins was recorded in a 2×3 contingency table, in which rows were the control group and TFIIH, and columns were the three nominal categories of aligned number of amino acids. Observed frequency was written down. Expected frequencies were calculated for each cell by multiplying the corresponding vertical and horizontal totals and dividing by the grand total. The χ^2 statistic was calculated by using the indicated formula. There are 2 df for a 2×3 table. Values for χ^2 for 2 df are tabulated to be 5.99 and 9.21 for $P = 0.05$ and $P = 0.01$, respectively. The obtained value (9.939) was found to exceed both tabulated values of χ^2. This indicates that the probability of obtaining our calculated value by chance is smaller than 0.01, and therefore the null hypothesis is considered false at that P value, and we conclude that the presence of motives in TFIIH proteins does not arise by chance but it is different from that seen in a randomly taken population of similarly conserved proteins.

1. Lisby M, Mortensen UH, Rothstein R (2003) Colocalization of multiple DNA double-strand breaks at a single Rad52 repair centre. *Nat Cell Biol* 5:572–577.
2. Jimeno S, Rondón AG, Luna R, Aguilera A (2002) The yeast THO complex and mRNA export factors link RNA metabolism with transcription and genome instability. *EMBO J* 21:3526–3535.
3. Liu JW, Picard D (1998) Bioactive steroids as contaminants of the common carbon source galactose. *FEMS Microbiol Lett* 159:167–171.
4. Picard D, et al. (1990) Reduced levels of hsp90 compromise steroid receptor action in vivo. *Nature* 348:166–168.
5. Fasullo MT, Davis RW (1987) Recombinational substrates designed to study recombination between unique and repetitive sequences in vivo. *Proc Natl Acad Sci USA* 84:6215–6219.
6. Chávez S, Aguilera A (1997) The yeast HPR1 gene has a functional role in transcriptional elongation that uncovers a novel source of genome instability. *Genes Dev* 11:3459–3470.
7. Moriel-Carretero M, Aguilera A (2010) A postincision-deficient TFIIH causes replication fork breakage and uncovers alternative Rad51- or Pol32-mediated restart mechanisms. *Mol Cell* 37:690–701.
8. Rigaut G, et al. (1999) A generic protein purification method for protein complex characterization and proteome exploration. *Nat Biotechnol* 17:1030–1032.
9. Kainov DE, Vitorino M, Cavarelli J, Poterszman A, Egly JM (2008) Structural basis for group A trichothiodystrophy. *Nat Struct Mol Biol* 15:980–984.
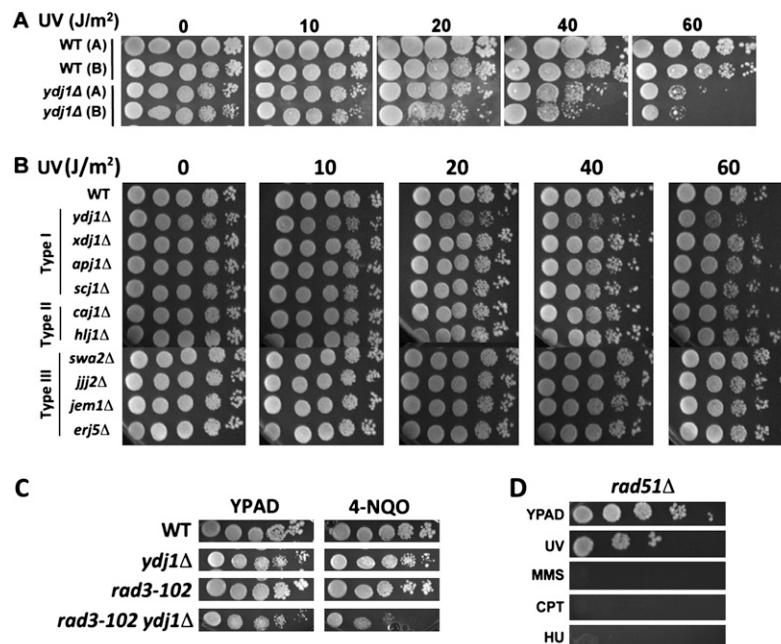
Fig. S1. Cells lacking Ydj1 are sensitive to UV-like DNA damage. (*A*) Serial dilutions of WT and *ydj1*Δ strains exponential cultures were plated on rich YPAD medium and irradiated with different UV doses. (*B*) Response to UV of mutants lacking chaperones of the Hsp40 group of type I, II, or III in comparison with WT and *ydj1*Δ strains. Strains were chosen because the lacking protein normally has a subcellular localization similar to that of Ydj1. Serial dilutions of cultures were plated on rich YPAD medium and irradiated with different UV doses. (*C*) Serial dilutions of WT, *ydj1*Δ, *rad3-102*, and their corresponding double mutant strains exponential cultures were plated on rich YPAD medium containing or not 0.01 mg/L 4-nitroquinolineoxide (4-NQO). (*D*) Tenfold serial dilution assays to establish *rad51*Δ sensitivity to various DNA damaging agents. Doses used are 60 J/m² UV, 0.01% MMS, 10 μg/mL CPT, and 50 mM HU.
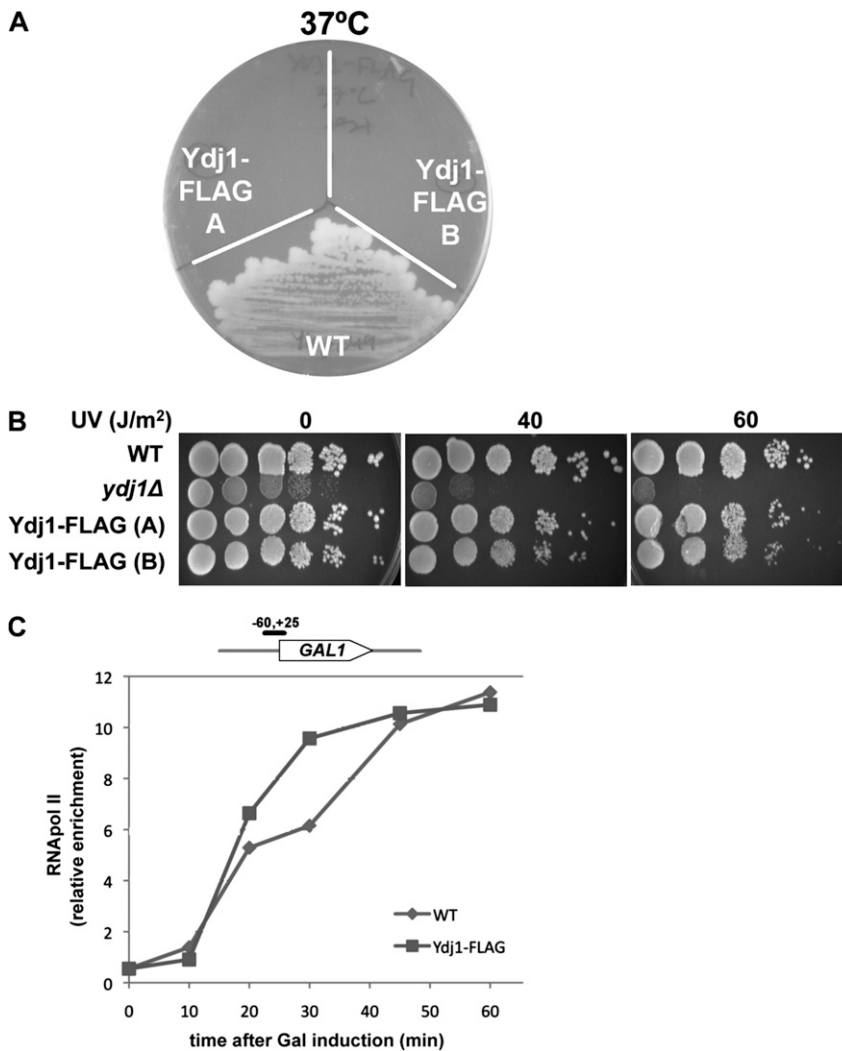
Fig. S2. Ydj1-FLAG strains tagged at the protein C-terminal region are proficient in TFIIH functions. (*A*) Growth of WT and C-terminal-tagged Ydj1-FLAG strains at 37 °C on rich YPAD medium. (*B*) Serial dilutions of WT, *ydj1Δ*, and C-terminal-tagged Ydj1-FLAG exponential cultures irradiated with different UV doses. (*C*) Chromatin immunoprecipitation with anti-RNAPII antibody 8WG16 in Ydj1-FLAG and WT strains. Recruitment was studied at the *GAL1p* upon galactose activation. Other details are as in Fig. 2*D*.
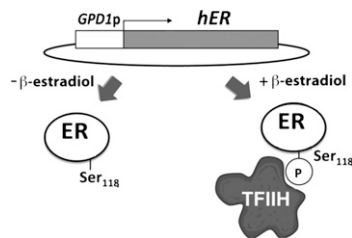

Fig. S3. The human estrogen inducible system transplanted into yeast. The human ER gene is under the control of the yeast *GPD1* constitutive promoter. Upon estrogen addition, TFIIH phosphorylates Ser118 in the ER protein, which then can bind to EREs.
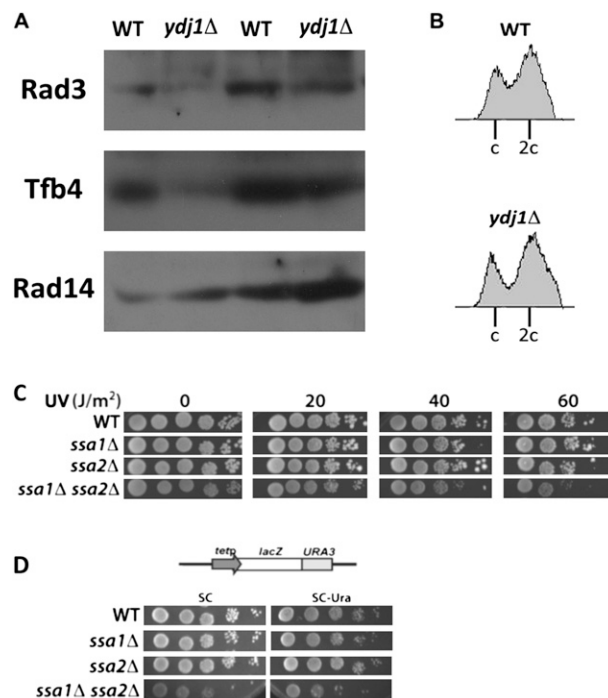
Fig. S4. TFIIH stoichiometry is altered upon removal of chaperone network members. (*A*) Immunodetection of Tfb4 (using anti-Tfb4; gift from Yuichiro Takagi, Indiana University, Indianapolis, IN) and Rad3 (using sc-11963) in WT and in *ydj1Δ* crude extracts from cells grown to exponential phase in SC. Rad14 detection is shown as a control of the NER-independent TFIIH-specific decrease seen in *ydj1Δ* cells for TFIIH components. Two independent experiments are shown in the same gel. (*B*) FACS patterns of exponentially growing WT and *ydj1Δ* cells in SC medium. Single and double DNA content are indicated by "c" and "2c," respectively. (*C*) Serial dilutions of exponential cultures from WT, *ssa1Δ*, *ssa2Δ*, and their corresponding double mutant strains plated on YPAD and irradiated with different UV doses. (*D*) Gene expression assay using the pLAUR system. Serial dilutions were made from exponential cultures of WT, *ssa1Δ*, *ssa2Δ*, and their corresponding double mutants. Transformants were selected in SC-his. Growth in SC-his-ura serves as a measure of pLAUR expression and transcription.

A

Category	Protein	Number of conserved consensus motifs	annealing aa	% identity	% similarity	identical aa	similar aa
A	Tfb5/TTDA	1	67	28.4	76.1	19.028	50.987
B	Tfb4/p34	1	321	30.5	64.2	97.905	206.082
C	Ssl1/p44	1	394	39.1	66.5	154.054	262.01
D	Tfb2/p52	3	508	34.6	64.2	175.768	326.136
E	Rad3/XPD	1	755	52.5	81.7	396.375	616.835
F	Rad25/XPB	1	794	53	77.7	420.82	616.938
		Σ 8				1263	2078
A	Got1/GOLT1B	0	119	43.7	75.6	52.003	89.964
B	Mvp1/SNX8	0	352	25.9	60.8	91.168	214.016
C	Aat2/GOT1	2	412	46.6	71.6	191.992	294.992
D	Rad2/XPG	0	1061	26.2	60.1	277.982	637.661
E	Rli1/ABCE1	3	605	68.4	87.6	413.82	529.98
F	Mcm7/MCM7	4	773	45.8	72.2	354.034	558.106
		Σ 9				1380	2324
A	Thp1/PCID2	0	181	27.1	63.5	49.051	114.935
B	Bim1/MAPRE1	0	278	35.3	60.4	98.134	167.912
C	Sec13/SEC13	0	302	50.7	76.5	153.114	231.03
D	Ste7/MAP2K1	1	396	35.1	64.1	138.996	253.836
E	Rad54/RAD54L	2	618	49.8	74.9	307.764	462.882
F	Pmr1/ATP2C1	5	927	49.4	77.8	457.938	721.206
		Σ 8				1204	1951
A	Tom20/TOMM20	0	141	27	59.6	38.07	84.036
B	Adh1/ADH1C	0	358	27.4	56.1	98.092	200.838
C	Cys3/CTH	0	393	51.1	77.4	200.823	304.182
D	Esa1/KAT5	2	512	41.2	63.1	210.944	323.072
E	Acs1/ACSS1	3	663	46	72.9	304.98	483.327
F	Sdh1/SDHA	4	660	63.5	83.5	419.1	551.1
		Σ 9				1272	1946

B

motif frequency	protein classes			
	<300 aa	300-600 aa	>600 aa	total
TFIIH	O=1	O=5	O=2	8
	E=0.235	E=2.353	E=5.418	
controls	O=0	O=5	O=21	26
	E=0.76	E=7.65	E=17.59	
total	1	10	23	34

χ^2	protein classes			
	<300 aa	300-600 aa	>600 aa	total
TFIIH	2.49	2.978	2.132	
controls	0.76	0.918	0.661	
total				9.939

$$\chi^2 = \frac{\Sigma\,(\,O - E\,)^2}{E}$$

	P	$\chi^2_{(df=2)}$
	0.05	5.99
	0.01	9.21

Fig. S5. Statistical significance of the Ydj1-binding consensus presence in TFIIH components. (*A*) Random selection of proteins sharing resembling identity, similarity and aligned amino acids scores with those of TFIIH proteins when comparing human and yeast sequences were assigned a category from A to F and randomly combined in three control groups. The number of conserved Ydj1-binding consensus motifs was then counted. (*B*) The number of conserved motifs found in control groups and in TFIIH proteins, classified by length, was recorded in a 2 × 3 contingency table. Observed (O) and expected (E) frequencies are indicated. The χ^2 statistic was calculated by using the indicated formula. The obtained value was found to exceed the tabulated value of χ^2 for $P = 0.05$ and $P = 0.01$.

Table S1. TFIIH defects associated with mutations in the Ydj1-binding consensus motif

Protein	Organism	Mutation	Phenotype	Ref.
Rad25/XPB	*H. sapiens*	S 751E	No 5′ incision by ERCC1/XPF during NER if constitutively phosphorylated	1
Tfb2/p52	*H. sapiens* D. melanogaster	Δ202–462	No XPB retention	2
Tfb2/p52	*H. sapiens* D. melanogaster	Δ393–462	No Tfb5 binding; leads to NER defects	2
Tfb5/TTDA	*S. cerevisiae*	Δ1–14*	No Tfb2 binding; leads to NER defects	3, 4
Rad3/XPD	*H. sapiens*	G675R	No Ssl1 interaction; leads to XPCS	5
Ssl1/p44	*H. sapiens*	Δ252–395	No p34 interaction; leads to transcription defects	6
Tfb4/p34	*H. sapiens*	Δ1–242	No interaction with p44; leads to transcription defects	7

*Tfb5Δ1–7 has no detectable phenotype.

1. Coin F, et al. (2004) Phosphorylation of XPB helicase regulates TFIIH nucleotide excision repair activity. *EMBO J* 23:4835–4846.
2. Fregoso M, et al. (2007) DNA repair and transcriptional deficiencies caused by mutations in the Drosophila p52 subunit of TFIIH generate developmental defects and chromosome fragility. *Mol Cell Biol* 27:3640–3650.
3. Kainov DE, Vitorino M, Cavarelli J, Poterszman A, Egly JM (2008) Structural basis for group A trichothiodystrophy. *Nat Struct Mol Biol* 15:980–984.
4. Zhou Y, Kou H, Wang Z (2007) Tfb5 interacts with Tfb2 and facilitates nucleotide excision repair in yeast. *Nucleic Acids Res* 35:861–871.
5. Coin F, et al. (1998) Mutations in the XPD helicase gene result in XP and TTD phenotypes, preventing interaction between XPD and the p44 subunit of TFIIH. *Nat Genet* 20:184–188.
6. Fribourg S, et al. (2000) Structural characterization of the cysteine-rich domain of TFIIH p44 subunit. *J Biol Chem* 275:31963–31971.
7. Fribourg S, et al. (2001) Dissecting the interaction network of multiprotein complexes by pairwise coexpression of subunits in E. coli. *J Mol Biol* 306:363–373.

Table S2. Strains used in this work

Name	Genotype	Source
YBP249	*MAT**a** ade2-1 can1-100 his3-11,15 leu2-3,112 trp1-1 ura3-1 bar1Δ RAD5*	B. Pardo (CABIMER, Seville, Spain)
YBP250	*MATα ade2-1 can1-100 his3-11,15 leu2-3,112 trp1-1 ura3-1 bar1Δ RAD5*	B. Pardo (CABIMER, Seville, Spain)
Y03012	*MAT**a** his3D1 leu2Δ0 met15D0 ura3Δ0 ydj1Δ::KAN*	EUROSCARF
MMI-81	*MATα ade2-1 can1-100 his3-11,15 leu2-3,112 trp1-1 ura3-1 RAD5 rad3-102::HYG*	1
WSR51	*MAT**a**-inc ade2-1 trp1-1 ura3-1 his3-11,15 leu2::SFA can1- 100 ade3::GAL1-HO rad51Δ::KAN*	2
WSR52	*MAT**a**-inc ade2-1 trp1-1 ura3-1 his3-11,15 leu2::SFA can1- 100 ade3::GAL1-HO rad52Δ::KAN*	2
YNN299	*MAT**a** his3Δ200 ura3-1 lys2-801 ade2-101 his3-Δ3′-his3-Δ5′:: URA3*	3
SC0946	*MAT**a** ade2 arg4 leu2-3,112 trp1-289 ura3-52 RAD3- TAP::HIS3*	EUROSCARF
MMIV-5	*MAT**a** ade2 arg4 leu2-3,112 trp1-289 ura3-52 RAD3- TAP::HIS3 ydj1Δ::NAT*	Present study
MMIV-17	*MAT**a** ade2-1 can1-100 his3-11,15 leu2-3,112 trp1-1 ura3-1 bar1Δ RAD5 YDJ1-FLAG::KAN*	Present study
HQY957	*MAT**a** his3Δ1 leu2Δ0 met15Δ0 ura3Δ0 kin28Δ::KAN [LEU2 KIN28-HA]*	4
HQY958	*MAT**a** his3Δ1 leu2Δ0 met15Δ0 ura3Δ0 kin28Δ::KAN [LEU2 KIN28-ts16-HA]*	4
Y07202	*MAT**a** his3Δ1 leu2Δ0 met15Δ0 ura3Δ0 trp1Δ::KAN*	EUROSCARF
MMHQY957	*MAT**a** his3Δ1 leu2Δ0 met15Δ0 ura3Δ0 trp1Δ::KAN kin28Δ::KAN [LEU2 KIN28-HA]*	Present study
MMHQY958	*MAT**a** his3Δ1 leu2Δ0 met15Δ0 ura3Δ0 trp1ΔKAN kin28ΔKAN [LEU2 KIN28-ts16-HA]*	Present study
CB010-TFB4	*MAT**a** pep4::HIS3 prb1::LEU2 prc1::HISG can1 ade2 trp1 ura3 his3 leu2-3,112 TFB4-TAP::TRP1*	5
MMIII-60(P4)	*MAT**a** pep4::HIS3 prb1::LEU2 prc1::HISG can1 ade2 trp1 ura3 his3 leu2-3,112 TFB4-TAP::TRP1 ydj1Δ::NAT*	Present study
Y 02701	*MAT**a** his3D1 leu2Δ0 met15D0 ura3Δ0 xdj1Δ::KAN*	EUROSCARF
Y 02999	*MAT**a** his3D1 leu2Δ0 met15D0 ura3Δ0 apj1Δ::KAN*	EUROSCARF
Y 00800	*MAT**a** his3D1 leu2Δ0 met15D0 ura3Δ0 scj1Δ::KAN*	EUROSCARF
Y 00183	*MAT**a** his3D1 leu2Δ0 met15D0 ura3Δ0 caj1Δ::KAN*	EUROSCARF
Y 00744	*MAT**a** his3D1 leu2Δ0 met15D0 ura3Δ0 hlj1Δ::KAN*	EUROSCARF
Y 03679	*MAT**a** his3D1 leu2Δ0 met15D0 ura3Δ0 swa2Δ::KAN*	EUROSCARF
Y 01263	*MAT**a** his3D1 leu2Δ0 met15D0 ura3Δ0 jjj2Δ::KAN*	EUROSCARF
Y 01350	*MAT**a** his3D1 leu2Δ0 met15D0 ura3Δ0 jem1Δ::KAN*	EUROSCARF
Y 05855	*MAT**a** his3D1 leu2Δ0 met15D0 ura3Δ0 erj5Δ::KAN*	EUROSCARF

EUROSCARF, EUROpean Saccharomyces Cerevisiae ARchive for Functional Analysis.

1. Moriel-Carretero M, Aguilera A (2010) A postincision-deficient TFIIH causes replication fork breakage and uncovers alternative Rad51- or Pol32-mediated restart mechanisms. *Mol Cell* 37:690–701.
2. González-Barrera S, García-Rubio M, Aguilera A (2002) Transcription and double-strand breaks induce similar mitotic recombination events in Saccharomyces cerevisiae. *Genetics* 162:603–614.
3. Fasullo MT, Davis RW (1987) Recombinational substrates designed to study recombination between unique and repetitive sequences in vivo. *Proc Natl Acad Sci USA* 84:6215–6219.
4. Qiu H, Hu C, Wong CM, Hinnebusch AG (2006) The Spt4p subunit of yeast DSIF stimulates association of the Paf1 complex with elongating RNA polymerase II. *Mol Cell Biol* 26:3135–3148.
5. Borggrefe T, Davis R, Bareket-Samish A, Kornberg RD (2001) Quantitation of the RNA polymerase II transcription machinery in yeast. *J Biol Chem* 276:47150–47153.